Electronic Supplementary Information

Double signal amplification based on palladium nanoclusters and nucleic acid cycles on μPAD for dual-model detection of microRNAs

Xuemei Yin[a], Linlin Liang[a,b], Peini Zhao[a], Feifei Lan[a], Lina Zhang[c*], Shenguang Ge[b*] and Jinghua Yu[a]

[a]*School of Chemistry and Chemical Engineering, University of Jinan, Jinan 250022, P.R. China*

[b]*Institute for Advanced Interdisciplinary Research, University of Jinan, Jinan 250022, P.R. China*

[c]*Shandong Provincial Key Laboratory of Preparation and Measurement of Building Materials, University of Jinan, Jinan 250022, P.R. China*

*Corresponding author: Lina Zhang and Shenguang Ge

E-mail: mse_zhangln@ujn.edu.cn

E-mail: chm_gesg@163.com

Fabrication and characterization of the μPAD

The μPAD was created using a previously reported method with large modification, and a detailed procedure was described below. Firstly, we selected whatman chromatography paper #1 (GE Healthcare Worldwide) which was adjusted to A4 size as the substrate material. Then, Adobe Illustrator CS4 software was employed to create the shape of hydrophobic barrier on origami device. Subsequently, a commercially available solid-wax printer (FUJIXEROX Phaser 8560DN, Japan) was used to put the wax on an A4 #1 paper as the insulation agent (Fig. S1). Finally, the wax-printed paper sheet was baked in an oven at 130 ºC for about 150 s to make the printed wax melt and penetrate through the paper to form the hydrophobic and insulating patterns (Fig. S2, S3). This origami device was comprised of a reaction zone, a fluorescent detection zone and a colorimetric detection zone (Fig. S4A). The paper sheet was cut into individual origami μPAD for further modification and employment (Fig. S4B-D).

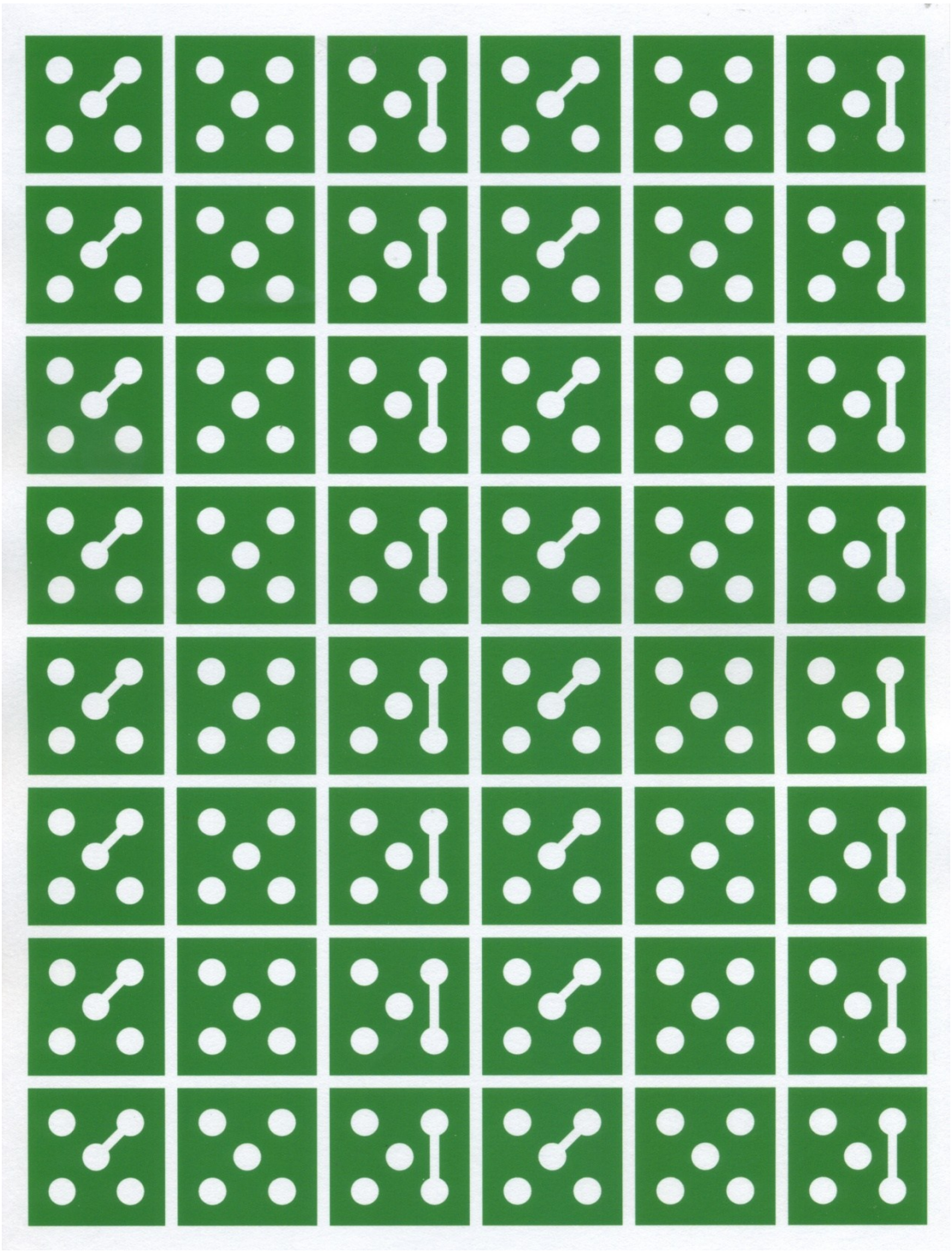

Fig. S1 Paper sheets were firstly patterned in bulk using a wax printer.

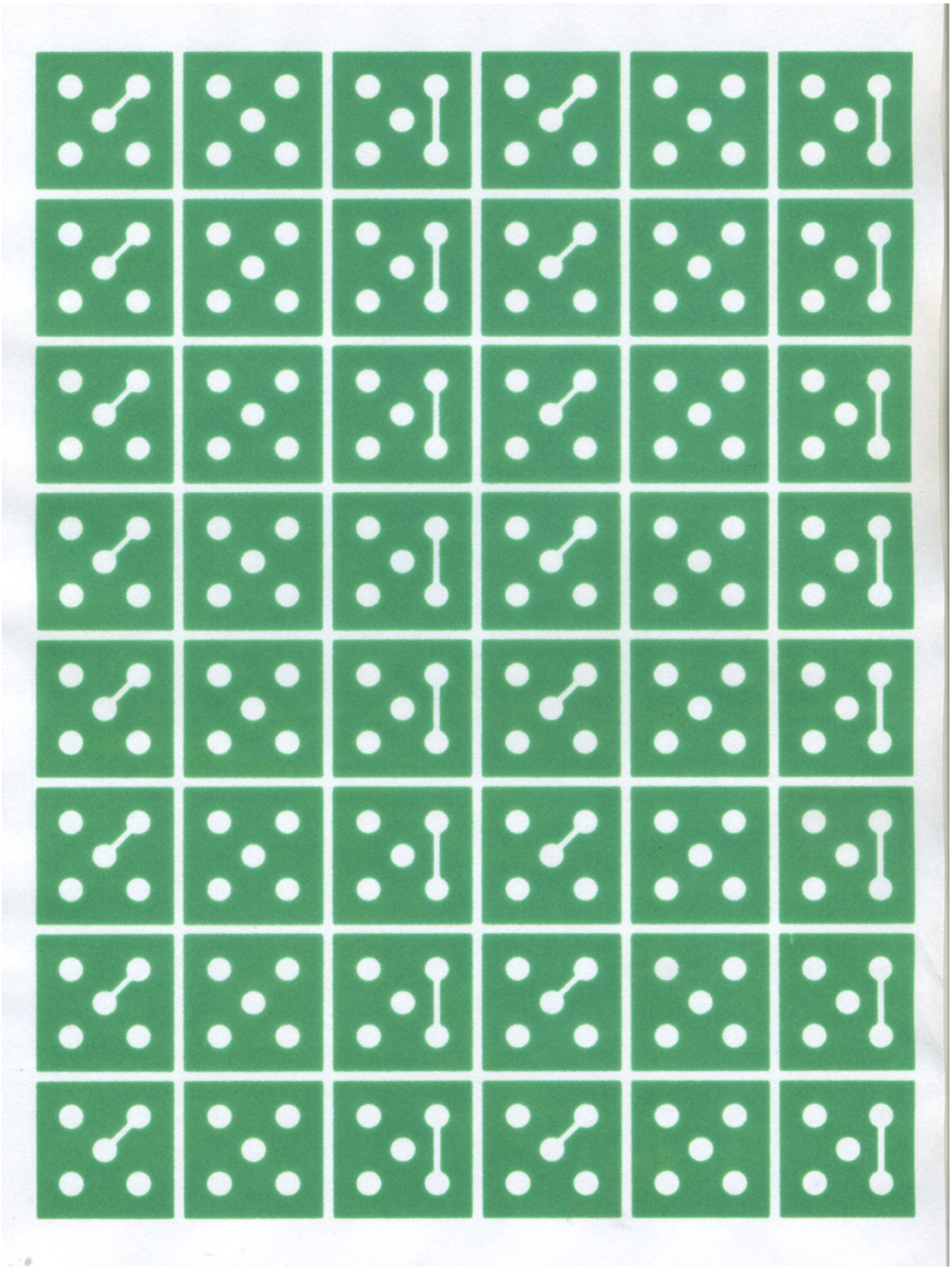

Fig. S2 Wax-patterns of the μPAD on a paper sheet (A4) after baking.

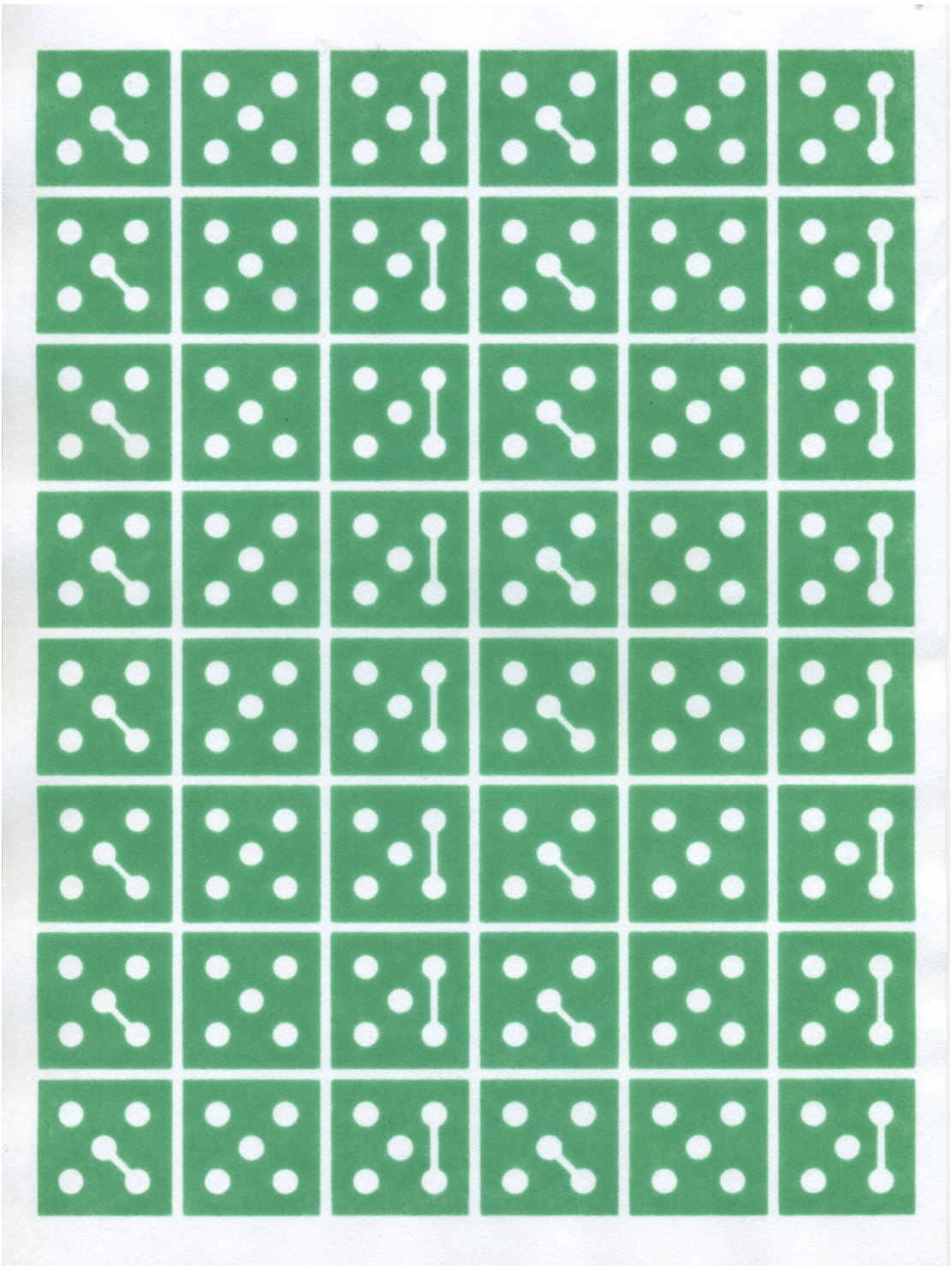

Fig. S3 Wax-patterns of the μPAD on a paper sheet (A4) after baking on the reverse side of Fig. S2.

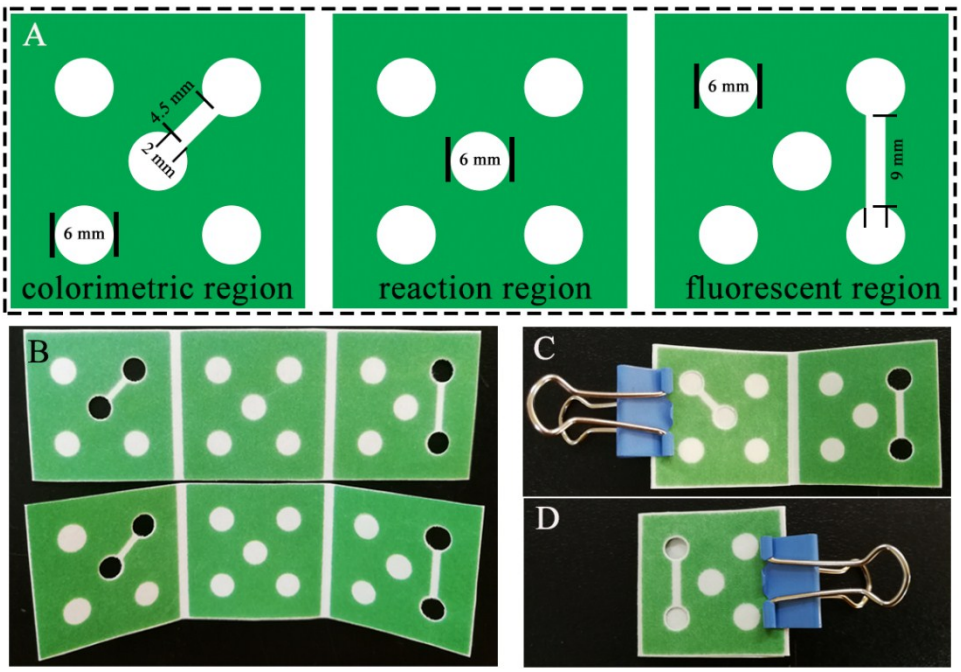

Fig. S4 Working regions of the μPAD.

The preparation and characterization of Pt-μPAD

The influence of the selection of different reductants and the reactant proportion on the growth of Pt NPs on the μPAD were received on the Fig. S5 and S6. As showed in the Fig. S5, compared with the bare μPAD (Fig. S5A), when ascorbic acid (Fig. S5B) and hydroxylamine hydrochloride (Fig. S5C) served as the reducing agent, Pt NPs grew less on the surface of the μPAD, especially for ascorbic acid, there was almost no Pt NPs. However, with $NaBH_4$ as reducing agent, H_2PtCl_6 could be commendably reduced to generate Pt NPs with the uniform particles and consistent thickness which was conducive to further research. Based on the analysis above, $NaBH_4$ was chosen as the optimum reducing agent for the preparation of Pt-μPAD.

With $NaBH_4$ as the reducing agent, the amount and proportion of $NaBH_4$ and H_2PtCl_6 were studied. Figure S6 showed that there was homogenous growth for Pt NPs

when the ratio of $NaBH_4$ and H_2PtCl_6 was 1. For further study, in comparison with the dosage of 50 μL (Figure S6A), 100 μL was chosen as the optimal dosage for the growth of Pt NPs on μPAD in this study (Figure S6B). C and D of Figure S6 showed that the bigger ratio was, the more serious cracks appeared. Taking the above result into account, the choice of $NaBH_4$ and H_2PtCl_6 was both 50 μL to develop Pt NPs on the μPAD.

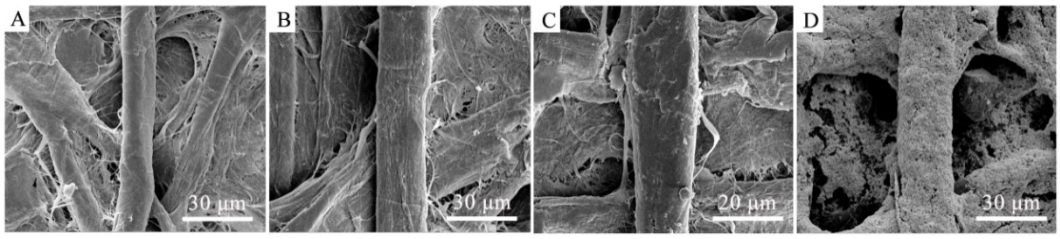

Fig. S5 SEM images of (A) bare paper, (B) ascorbic acid, (C) hydroxylamine hydrochloride, (D) $NaBH_4$

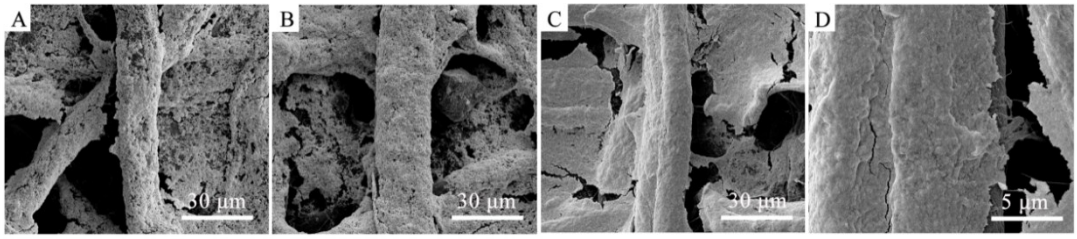

Fig. S6 SEM images of (A) 1:1 of 50 μL, (B) 1:1 of 100 μL, (C) 2:1 of 100 μL, (D) 3:1 of 100 μL

Optimization of the main experimental conditions

In our work, DNA-Pd NCs, as a kind of fluorescent agent, were superior to organic dyes, and g-C_3N_4 NSs could act as an efficient fluorescence quencher based on the photoinduced electron transfer mechanism or energy transfer mechanism. Therefore, we firstly evaluated the fluorescence quenching capability upon different volume of the prepared g-C_3N_4 NSs. As shown in Figure S7A, the fluorescence spectra in the presence

of different level of g-C_3N_4 NSs was received. The image showed that fluorescence intensity of Pd NCs gradually decreased with the increase of the volume of g-C_3N_4 NSs, which indicated that Pd NCs were adsorped on the surface of g-C_3N_4 NSs efficiently. Among them, 100 μL g-C_3N_4 NSs (2 mg/mL) could achieve to quench almost the full fluorescence of Pd NCs. Therefore, in the subsequent detection of miRNAs, 100 μL g-C_3N_4 NSs were used for this research.

For acquiring the optimal analytical performance, the influence factors such as pH, temperature, and the concentration of H_2O_2 which peroxidase and mimetic peroxidase shared in commom, as well as incubation time were investigated, respectively. Firstly, the relation between the catalytic activity of Pd NCs and pH was studied in the range of pH 3.8-8.0. Figure S7B indicated the optimal catalytic activity of Pd NCs was obtained at pH 4.8. The effect of temperature on catalytic activity of the Pd NCs was studied in the range of 15 to 60 ºC, as shown in curve a of Figure S7C, the optimal catalytic temperature was about 28 ºC**.** In the following fluorescent and colorimetric measurements, the temperature also played an important part, curve b of Figure S7C showed that the oxidized product had slight characteristic absorbance with variation in temperature. From the above, to ensure the accuracy and convenience, we chose the room temperature as experimental temperature. The concentration of H_2O_2 would also produce an effect on the characteristic absorbance of the oxidized product, as shown in Figure S7D, within the scope of 0.5% to 3.5% (v/v), we obtained the maximum catalytic activity in 2 % of H_2O_2 with TMB arriving as a substrate. At last, we conducted a research about incubation time in the proposed biosensor influencing on experimental

performance. As showed in Figure S7E**,** the optimal incubation time was 40 min in the range of 10 min to 80 min.

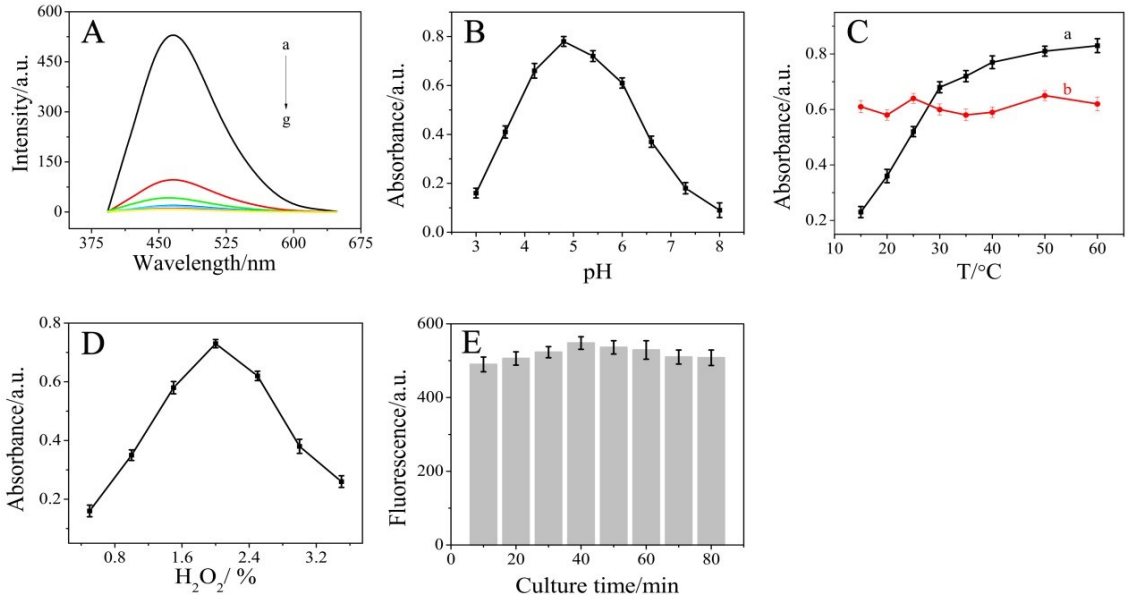

Fig. S7 Effectd of the quencher (A), the pH (B), the temperature (C), the H_2O_2 (D), and the incubation time (E) on the property of proposed biosensor.

Calculating method of limit of detection (LOD)

According to the definition of detection limit in "IUPAC Compendium of Analytical Nomenclature", detection limit means that the lowest concentration or quality which could be detected and possessed distinguishing signal value compared with the blank solution. In this work, LOD expressed the lowest concentration derived from smallest measure that could be detected by our designed biosensor, and the equation displayed as below[1]:

$$S_t - S_b = 3\sigma$$

S_t represents the gross analysis signal, S_b represents the field blank signal, and σ represents the standard deviation of a blank solution (n=11).

The corresponding LOD expressed in concentration units is derived from the calibration function we have got: $\Delta I = 122.53 \times \lg [\text{let-7a}]\ (\mu M) + 1089.96$, and all the details are illustrated in table S1:

Table S1. Fluorescence intensity and corresponding information of field blank

Fluorescence intensity of field blank						Average Value	Standard Deviation	LOD
51.625	68.597	29.828	39.51	75.264	56.51	50.13	15.18	2.99 fM
62.213	31.426	52.663	49.852	33.96				

Table S2. Fluorescence intensity of miRNA with different concentration

c/μM	10^{-8}	10^{-7}	10^{-6}	10^{-5}	10^{-4}	10^{-3}
	129.74	297.23	409.2	557.03	615.1	765.3
I/a.u.	164.52	289.59	415.49	531.8	647	759.92
	141.75	271.85	391.65	540.97	642.64	783.06
Average/a.u.	145.34	286.22	405.45	543.27	634.91	769.43
Blank/a.u.				50.13		
ΔI/a.u.	95.2	236.1	355.3	493.1	584.8	719.3

Table S3. The comparison of different miRNAs detection methods

Method	Linear range/fM	Detection limit/fM	References
LC-MS/MS	10^3 to 10^8	1000	2
Electrochemistry	0.1 to 100	0.067	3
PEC	5 to 3000	2.26	4
Photoluminescence	1-60 miRNA copies	-	5
Simoa	0 to 1.5×10^6	500	6
Fluorescence	10 to 10^7	3	This work

LC-MS/MS: Liquid chromatography-tandem mass spectrometry

PEC: Photoelectrochemistry

Simoa: Single molecule arrays

Table S4 Recovery tests of let-7a in the human serum samples by the proposed biosensor and RT-PCR method

sample	add/pM	found/pM	recovery/%	RT-PCR/pM	recovery/%
serum	0.2	0.22	110.0	0.21	105.0
	1.0	0.91	91.00	0.94	94.00
	10.0	9.68	96.80	9.89	98.90
	100.0	99.23	99.23	99.54	99.54

References

1. D. MacDougall and W. B. Crummett, *Anal. Chem.*, 1980, **52**, 2242-2249.

2. F. Xu, T. Yang and Y. Chen, *Anal. Chem.*, 2016, **88**, 754-763.
3. J. Zhang, L. L. Wang, M. F. Hou, Y. K. Xia, W. H. He, A. Yan, Y. P. Weng, L. P. Zeng and J. H. Chen, *Biosens. Bioelectron.*, 2018, **102**, 33-40.
4. H. Yin, Y. Zhou, B. Li, X. Li, Z. Yang, S. Ai and X. Zhang, *Sens. Actuators, B: Chem.*, 2016, **222**, 1119-1126.
5. J. D. Harvey, P. V. Jena, H. A. Baker, G. H. Zerze, R. M. Williams, T. V. Galassi, D. Roxbury, J. Mittal and D. A. Heller, *Nat. Biomed. Eng.*, 2017, **1**, 697.
6. D. M. Rissin, B. Lopez-Longarela, S. Pernagallo, H. Ilyine, A. D. B. Vliegenthart, J. W. Dear, J. J. Diaz-Mochon and D. C. Duffy, *PLoS. One*, 2017, **12**, e0179669.